

AUTOMATIC TAKE-OFF AND LANDING OF A VERY LIGHT ALL ELECTRIC OPTIONALLY PILOTED AIRCRAFT

Simon Scherer¹, Moritz Speckmaier¹, Daniel Gierszewski¹, Chinmaya Mishra¹, Agnes Steinert¹, Rasmus Steffensen¹, Simona Wulf¹ & Florian Holzapfel¹

¹Technical University of Munich, TUM School of Engineering and Design, Department of Aerospace and Geodesy, Institute of Flight System Dynamics

Abstract

This paper describes the development, testing and demonstration of an automatic take-off and landing (ATOL) system for a very light all-electric optionally-piloted aircraft. The presented system allows to automatically control the aircraft during approach, flare and take-off flight phases. The ATOL system utilizes the existing automatic flight control system (AFCS) of the demonstrator aircraft and provides additional mode logics, autopilot controller commands and state limits as well as additional functions specific for automatic take-off and landing. The landing is performed by the aircraft following a pre-defined landing trajectory and vertical speed control during the flare. To account for crosswind conditions, a decrab maneuver is conducted prior to touch down. The take-off is conducted based on a pre-defined sequence for acceleration during take-off run, rotation and initial climb segments. Functional algorithms were designed and tested using software and aircraft-in-the-loop simulations, respectively. The functions required for ATOL such as the flare or pitch control modes were initially flight tested in a safe altitude. Simulation results as well as real flight test data is shown for an automatic take-off and landing of the demonstrator aircraft.

Keywords: Automatic take-off, Automatic landing, Electric aircraft, Very light aircraft, Optionally piloted vehicle

Nomenclature

AIL	=	Aircraft-in-the-Loop
ATOL	=	Automatic Take-off and Landing
AFCS	=	Automatic Flight Control System
AFGCS	=	Automatic Flight Guidance and Control System
FCC	=	Flight Control Computer
FDM	=	Flight Dynamics Model
FMC	=	Flight Management Computer
GCS	=	Ground Control Station
IAS	=	Indicated Airspeed
ILS	=	Instrument Landing System
OPV	=	Optionally-piloted Aircraft
SIL	=	Software-in-the-Loop
WoW	=	Weight-on-Wheels

1 Introduction

Automatic landing systems are widely used for large CS-25 aircraft. Different categories of systems have different decision heights, up to which the pilot needs to take over control for the final landing. Only CAT IIIc systems support automatic landing including touch-down and roll-out [1]. Current automatic landing systems onboard aircraft rely on ground based infrastructure such as an instrument

landing system (ILS). Such infrastructure is expensive and only available at large airfields. Further developments toward satellite based landing systems, which are cheaper and can be used for all runway directions, allow new and more efficient approaches. Honeywell for example developed a certified ground-based augmentation system for CAT I [2].

Beside the current standard autoland systems based on an ILS, recent research has extended the capabilities of ATOL systems. Airbus has demonstrated automatic taxiing, take-off and landing (*ATTOL*) on an *Airbus A350* using image recognition technology [3]. Autoland capabilities are also increasingly being used in general aviation. *Garmin* developed an emergency landing system for general aviation aircraft, which is able to proceed the flight to the closest possible airfield and perform automatic landing including roll-out in case the pilot is unable to fly [4]. *Xwing* demonstrated a fully autonomous gate-to-gate flight with an *Cessna 208B Grand Caravan*, including automatic taxiing, take-off and landing [5]

Automatic take-off and landing was also demonstrated independent within multiple research projects. Lamp et. al. developed a flight control system including automatic landing for a high-aspect-ratio aircraft [6]. Pinchetti et. al. demonstrated ATOL with a *Diamond Aircraft DA-42* general aviation aircraft [7]. Also previous work at the Institute of Flight System Dynamics of the Technical University of Munich independently demonstrated automatic landing and take-off for a *Diamond Aircraft DA-42* [8, 9] as well as for an unmanned aircraft with 150 kg [10].

In this paper, an ATOL system was adapted for an all electric very light aircraft. The system is based on an existing AFCS of the demonstrator aircraft, which provides autopilot and trajectory control functionalities. Additional functional algorithms for automatic take-off and landing are designed and implemented based on modular ATOL functions available from previous projects at the institute. Subsequent simulation and flight testing of required control functions were performed and the automatic take-off and landing was demonstrated in flight tests.

This paper is structured as follows. Section 2 introduces the demonstrator aircraft and gives an overview on the automatic flight guidance and control system (AFGCS) which was utilized for the automatic take-off and landing. The modifications and adaption of the ATOL system were described in section 3. Simulation results for testing and validation of the system are presented in section 4. Finally, section 5 shows flight test results of an automatic take-off and landing maneuvers of the demonstrator aircraft. Section 6 concludes the paper.

2 Demonstrator Aircraft

The functional algorithms for an Optionally piloted vehicle (OPV) were developed which include trajectory and autopilot control modes as well as functions for automatic take-off and landing. Therefore, a very-light all electric aircraft, based on a modified *PC-Aero Elektra One*, was used as demonstrator aircraft which is shown in figure 1. The aircraft has a wing span of 11 m and a maximum take-off weight (MTOW) of approx. 350 kg.

Within a previous research project, an AFCS capable of autopilot and trajectory flight was developed and flight tested on the demonstrator aircraft. During a follow-up project, the flight control algorithms were then extended by functionalities for automatic take-off and landing in order to provide full OPV capability.

The demonstrator aircraft was equipped with electro-mechanical actuators for the primary control surfaces which were attached to a conventional mechanical flight control system with electro-mechanical clutches. For the autothrust, a small actuator was connected to the thrust lever. The AFCS can be engaged by the pilot through closing the actuator clutches or disengaged for manual control through a button on the pilot stick. The sensor setup comprises an air data, attitude and heading reference system including satellite navigation using satellite based augmentation system (SBAS), a radar altimeter and sensors for the aircraft systems such as position of the primary flight controls, the flaps position, the gear position and gear strut travel used for weight-on-wheels measurement. Two separate computation units were used for flight control and flight management. An interface of flight management computer interface allowed the remote operation and monitoring from a ground control station (GCS) via a data link.



Figure 1 – Demonstrator aircraft *ELIAS* [11]

2.1 Automatic Flight Control System

The flight control algorithms were based on the modular AFGCS architecture developed at the Institute of Flight System Dynamics. Due to its generic structure, a wide range of flight control functionalities can be adapted to different configurations. Figure 2 shows the available software modules.

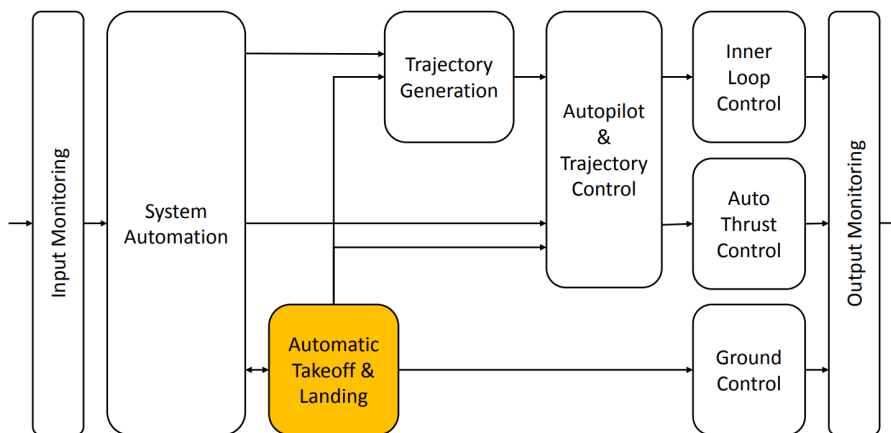


Figure 2 – Modular flight guidance and control system [9]

The different modules provide functionalities which are required for fully-automated flight control:

- Input monitoring
- System automation for mode and command selection and operation of secondary system
- Automatic take-off and landing
- Trajectory generation
- Trajectory control
- Autopilot for control of kinematic flight path and airspeed
- Autothrust for control of specific longitudinal force
- Inner-loop for control of body normal and lateral load specific force as well as bank angle

- Ground controller for aircraft control on ground
- Output monitoring

The AFGCS was successfully tested within multiple flight control applications, e.g. the institutes research aircraft *DA-42 MPP NG* and a novel UAV demonstrator [8, 9, 12, 13, 14, 15].

The intended operations of the demonstrator aircraft required only a subset of the available control modes of the AFGCS. The realized AFCS allow the control of airspeed by thrust or pitch, heading or track, flight path angle and altitude including altitude changes with automatic capturing of the target altitude. Altitude changes could be performed using either a selected vertical speed or an open descent and climb maneuver. Further, lateral and vertical navigation along a trajectory defined by waypoints is supported.

The three-dimensional trajectory control algorithm of the AFGCS used in previous applications could not be used due to limited computational power of the flight control computer (FCC). Instead, a simplified trajectory generation module was developed which only supports straight line segments. The control of the trajectory is realized using the autopilot functions for ground track and flight path angle control as well as speed by thrust using the autothrust. The track command results from the direct-to track toward the next waypoint and a cross-track error correction. The flight path angle command is generated based on the altitude error and the remaining distance to the next waypoint.

2.2 Ground Control Station and Flight Management Computer

A GCS is used for remote control and monitoring of the aircraft from the ground via a data link. The operator interface provides displays for primary flight data and a moving map. The moving map further allows to create and modify waypoints or waypoint lists and to save or load the lists.

Mode commands and the corresponding target values for the autopilot as well as the waypoint lists are send from the GCS to the flight management computer (FMC) onboard the aircraft via a *STANAG 4586* interface. The FMC receives and decodes the messages and forward the data to the FCC. Both, the GCS and the FMC were developed by a project partners.

3 Design of Functions for Automatic Take-off and Landing

For the design and adaption of the automatic take-off and landing control functions, flight data from the demonstrator aircraft during manual take-off and landings were used. Furthermore the proposed procedures and control strategies were discussed with the test pilot.

3.1 System Automation, Mode Logic and Command Selection

The system automation manages the de-/activation of AFCS modules as well as controlling the different operating modes, e.g. autopilot modes, trajectory flight or ATOL. Apart from the system automation, there is an automation for engaging and disengages the AFCS via the electro-mechanical clutches described in [16]. The operator inputs are handled by the FMC. Since these functionalities are also included in the original system automation of the modular AFCS [17], a simplified version of the system automation was developed for the interaction with the FMC. Figure 3 schematically shows the system automation.

If the flight control system is activated on ground, the state *parking* is entered from the *init* state.

In case a valid take-off command, the state *atol-unconfirmed* is entered. The system continuously monitors, if the selected take-off maneuver is possible. If all monitoring conditions (see section 3.4) are met and the pilot activates the AFCS, the state *atol* is entered and the automatic take-off is executed. After reaching the desired cruise altitude, trajectory following is activated by entering the state *fmc-auto-mode*.

In case the AFCS is activated in air during manual flight, all internal states of the the system automation and thereby of the ATOL module are reset. Depending on the command either the state *fmc-direct-mode* is activated for autopilot operation or the state *fmc-auto-mode* is entered for waypoint flight and can switch from one to another during cruise flight.

The activation of the automatic landing is possible after a waypoint based initial approach, while the state *fmc-auto-mode* is active, as defined in section 3.5. In case the activation conditions are met, the

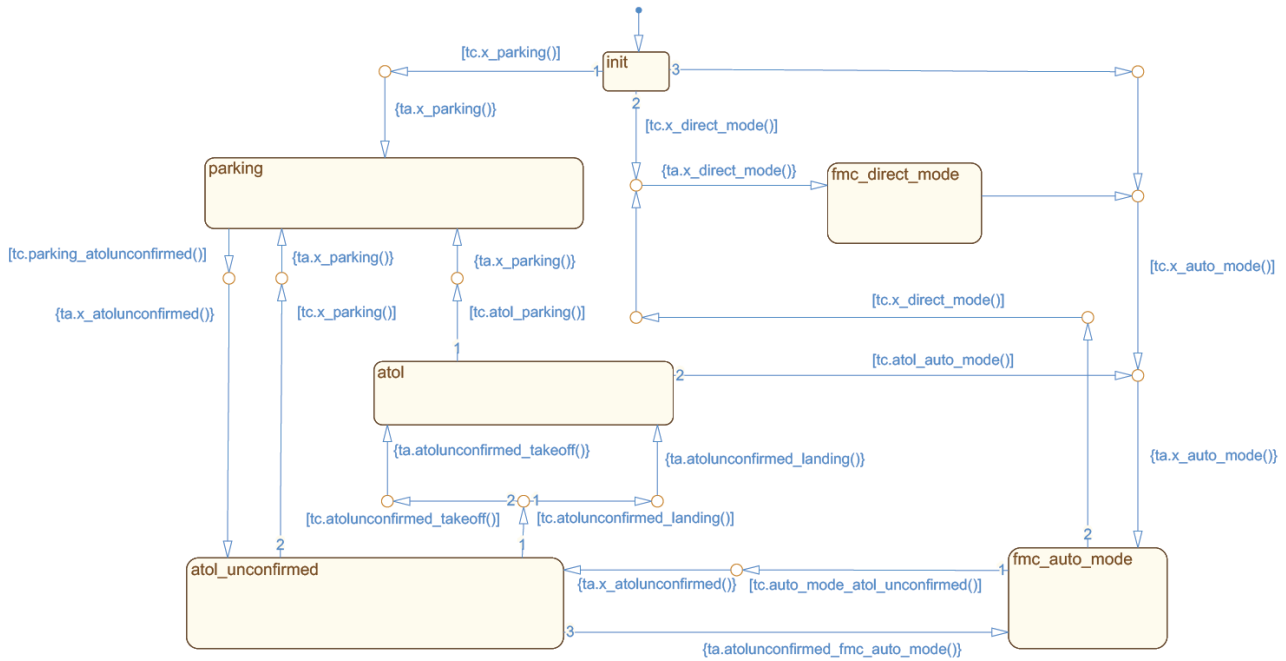


Figure 3 – Simple System Automation for ELIAS flight demonstrator

state *atol-unconfirmed* is entered. In case the ground station sends the correct activation command, the system automation enters the state *atol* and executes the automatic landing maneuver. After the roll-out, the state *parking* is entered.

3.2 Secondary Aircraft Controls and Systems

For full OPV operations, secondary aircraft systems such as the extension of flaps and gear or steering the aircraft on ground and braking need to be controlled automatically. Despite that the flaps and gear of the demonstrator aircraft were already operated electronically, these systems could not be controlled by the FCC due to missing interfaces. As a work-around, indications were displayed to the pilot when and how to operate these systems. The wheel brakes were operated hydraulically via differential pressure on the pilot pedals. Since no brake actuation system or anti-skid system, which are required for automatic braking, were available, the brakes were controlled only manually by the pilot. Further, the demonstrator aircraft was not equipped with a steerable nose wheel. Therefore, low speed directional control on ground was only possible by differential braking. Due to these limitations, aircraft control on ground such as taxiing, take-off run and braking after landing could only be done by the pilot.

3.3 Ground Controller

For the operation on ground such as take-off run and roll-out after touchdown, a dedicated ground controller was designed. This controller consists of three cascaded channels for roll, pitch and yaw rate as well as the corresponding roll, pitch and heading attitude angles.

The ground controller rate loops are based on a PI-controller structure while a proportional controller is used for the attitude loops. Dependent on the flight phase, the ground controller can be switched from attitude control to rate damping only.

When on ground during take-off run and roll out, the ground controller roll and pitch channel is used in damping mode. The integrators are disabled when the aircraft is on ground in order to avoid windup. The pitch controller is further used between flare and touchdown to control the pitch attitude in order to avoid a nose gear landing. The rotation prior to lift-off is also performed by the pitch ground controller.

For centerline tracking, the heading control loop is cascaded by two further loops for the lateral velocity and position error regarding the desired centerline track [18]. Since the demonstrator aircraft

does not allow for nose wheel steering or differential braking, low speed directional control was not possible. Therefore, the aircraft heading on ground needs to be controlled manually by the pilot. Due to safety reason, the rudder control remained inactive (clutch open) during take-off until lift-off and after touch-down in order to avoid a controller activation at high ground speed.

3.4 Take-Off Design

Procedure

The planned take-off procedure is shown in figure 4. For activation of the take-off, the aircraft must be on the desired runway threshold. Then the ground operator sends the command for take-off, which consist of the desired runway direction and the initial waypoint list for the subsequent cruise flight. The planned cruise trajectory consists of the waypoints *WP TO*, *WP Cruise Start* and *WP Cruise End*. The first Waypoint *WP TG active* is automatically generated by the AFCS using the current aircraft position, when the automatic take-off is activated. The requested take-off maneuver and the waypoints need to be confirmed by the pilot and are therefore shown on navigation display inside the aircraft cockpit.

Before activation of the request, the take-off monitoring of the ATOL module ensures that the aircraft states are within safe boundaries and sensors are operational. Therefore the position of the aircraft needs to be within boundaries along and across the runway centerline at the threshold. The aircraft is required to stand still with an orientation that is within a threshold for the selected runway heading. The roll and pitch attitude need to be within their respective threshold limits. Finally, the Weight-on-Wheels (WoW) sensors need to indicate that the aircraft is on ground. If all checks are passed, the take-off run can be activated by the pilot.

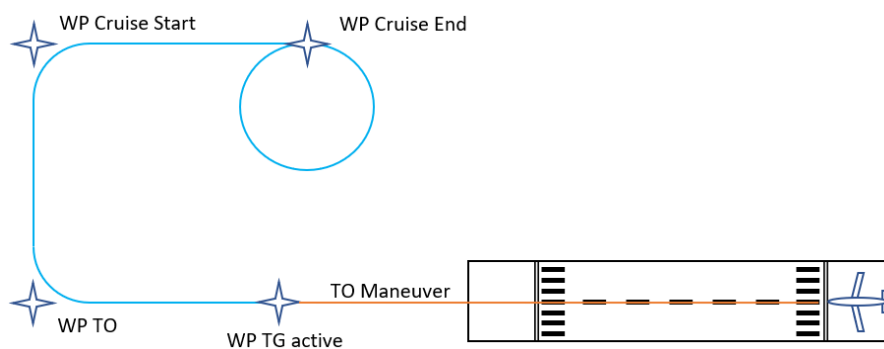


Figure 4 – Planned take-off procedure

Offline Trajectory Planning

The cruise trajectory after take-off was planned before flight and saved via a waypoint list on the GCS. In order to ensure safe initial climb, the first waypoint (*WP TO*) is placed in extension of the selected runway with a sufficient distance and altitude taking into account the aircraft climb performance. Upon reaching the first waypoint, the cruise trajectory is activated which consists of two right hand turns followed by a loiter waypoint at the end. The aircraft continues the loiter until a new waypoint list is uploaded to continue the flight.

Maneuver

The nominal take-off maneuver is divided into the following phases, which are controlled by a finite state machine:

Acceleration At activation, the aircraft thrust is set to maximum. During the acceleration phase the runway track angle is maintained by a center-line tracking controller using the rudder. The aileron and elevator are centered. When the rotation speed is reached, a feed-forward elevator rate command is added to initiate the rotation. In case the lift-off occurs before the rotation speed is reached, the ground pitch angle controller is activated and a predefined pitch angle is commanded, in order to

continue to accelerate close to ground. In that case, the ground bank angle controller is activated as well to maintain wings level.

Rotation and Lift-off When the pitch angle increases above a threshold, the rotation and lift-off phase is activated. Therefore, pitch controller is engaged to rotate the aircraft to a target pitch attitude of 5° with a constant pitch rate of 3 %/s. The roll controller is activated to maintain wings level.

Climb As soon as the height above ground reaches a threshold of 3 m and a positive rate of climb is established, the climb phase is activated. The control mode in the pitch axis changes from pitch command to speed by pitch to perform an open climb to a predefined cruise altitude with maximum thrust. The autopilot maintains the runway track. An indication to retract the landing gear is displayed to the pilot.

Cruise When the aircraft climbs above the cruise altitude, automatic take-off function is deactivated in order to continue the flight following the remaining waypoints. When activated, the trajectory generation uses the current aircraft position as the initial waypoint to calculate the trajectory to the next waypoint of the list. During cruise flight, new commands for the autopilot or another waypoint list can be sent by the operator via the GCS. If there is no new command, the aircraft loiters at the last waypoint.

Abort In order to abort the automatic take-off run, the pilot disengages the AFCS and manually takes over control of the aircraft.

3.5 Landing Design

Procedure

Figure 5 schematically shows the landing procedure. For the activation of the automatic landing maneuver, the operator sends a landing waypoint list and a standby go-around waypoint list in case of an aborted landing.

The first waypoint of the landing list is defined as a loiter waypoint (*WP LDG Request*) for confirmation of the landing. This waypoint furthermore contains the desired runway direction. Once the aircraft starts the loiter maneuver, the ground operator can confirm, that the landing is cleared and the aircraft continues to follow the waypoint list. The last two waypoints are designed to control the aircraft to the beginning of the parameterized landing trajectory (shown in orange) which is saved on the FCC.

In order to transition from the waypoint flight to following the landing trajectory, the aircraft position is checked to be within an virtual activation volume along with other safety requirements [19]. The used altitude reference is switched from barometric altitude (*QNH*) to orthometric height (*WGS84*) for the landing trajectory.

Offline Trajectory Planning

The initial approach and go-around trajectories are defined as waypoint lists, which are saved on the GCS and send to the aircraft when required. For each landing direction, a desired landing trajectory was generated using a custom toolbox. For efficient storage on the FCC, the trajectories are parameterized using a Bézier trajectory in a local runway coordinate frame [20]. Each landing trajectory was validated via simulation before flight.

Figure 6 shows a planned landing trajectory for the airfield *EDML* close to Munich. The waypoints of the initial approach are shown as white circles. The parameterized landing trajectory is shown in blue. Due to obstacle clearance and therefore altitude limitations, the descent angle for the final approach was set to 4° instead of a standard instrument landing glide slope of 3° .

Maneuver

The landing maneuver is divided into the following phases, which are controlled by a finite state machine.

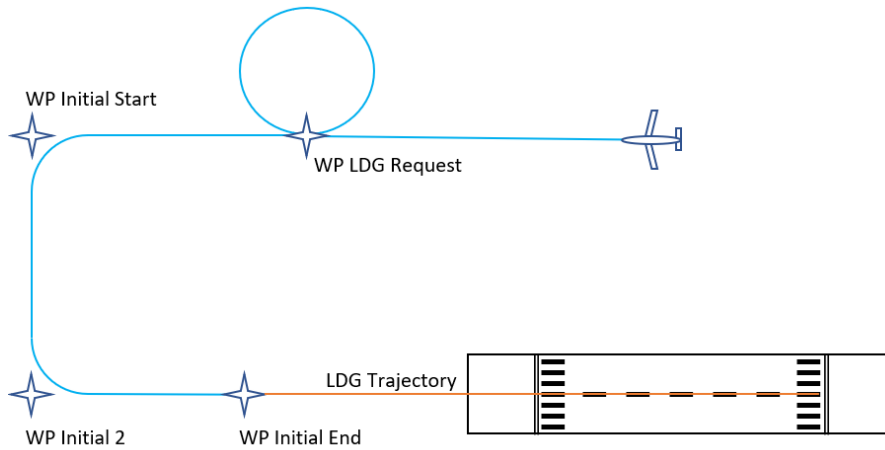


Figure 5 – Planned landing procedure

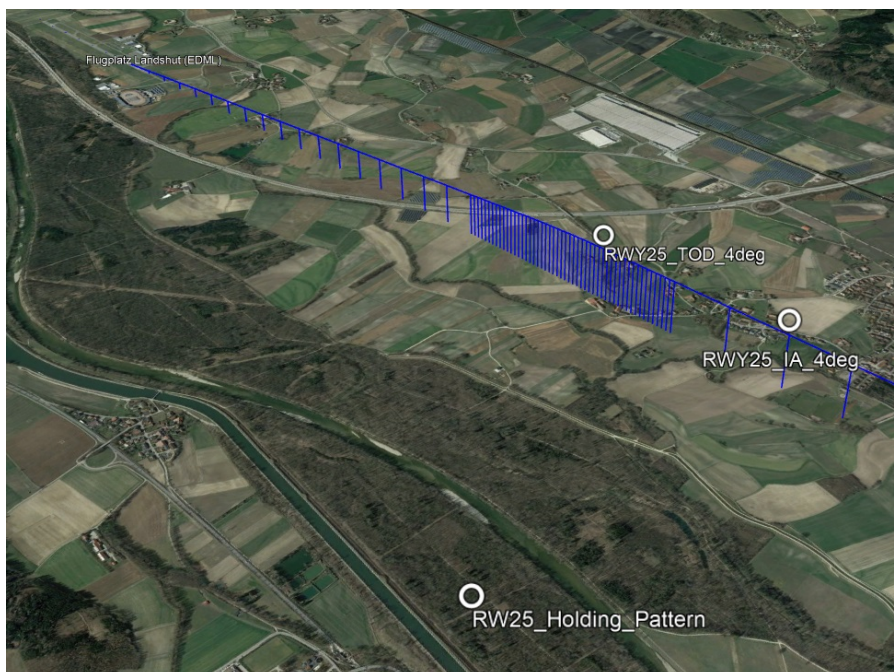


Figure 6 – Planned approach trajectory for EDML RWY 25

Intermediate and final approach The intermediate-approach phase covers the horizontal leg of the landing trajectory, which is followed by the trajectory controller. The airspeed is maintained by the autothrust controller. The progress along the trajectory is evaluated by mapping the current foot-point on the trajectory to an internal trajectory parameter. A jerk-free intercept to the descending leg is ensured by a smooth transition command. When the trajectory parameter indicates the descending leg, the final approach is activated. The final approach leg has a constant glide slope of 4° . The command for flaps out and gear out are displayed to the pilot during final approach.

Go-around During the intermediate and final approach, a go-around maneuver can either be activated by the autoland monitoring or the ground operator, in case a sensor failure or an unstable approach is detected. The go-around maneuver consists of two phases. In the first phase the thrust is set to maximum and the vertical load factor, bank angle and heading angle are stabilized. In the second phase the aircraft performs an open climb to cruise altitude while the track angle is hold constant to maintain the runway heading. After climbing to the cruise altitude, the system automation switches from ATOL to waypoint following as described in 3.1. The go-around waypoint list is activated and followed by the AFCS.

Based on the longitudinal position along the runway, the *WGS84* height is faded to height above ground based a complementary filtered radar altitude and vertical speed.

Flare The flare maneuver is activated based on a fixed height above ground. The vertical control changes from trajectory following to vertical speed control while simultaneously the indicated airspeed command is reduced linearly with height above ground. The flare law reduces the initial rate of descent to -0.3 m/s for touchdown. Initially, a command of 0 m/s is used to accelerate the aircraft response by generating lead in the command. As soon as the measured vertical speed reaches a threshold value, the target value of -0.3 m/s is commanded.

Pitch control and de-crab Just before touchdown, a pitch control phase is activated. Since the pitch attitude of the demonstrator aircraft in landing configuration is negative, the nose needs to be raised to avoid a nose gear landing. The initial command is set to the current pitch attitude at the activation of the pitch control phase. The pitch command is then linearly increased as the altitude above ground decreases. The minimum and maximum command values are furthermore saturated, to protect the pitch attitude close to ground. The thrust command is reduced to zero. In the lateral plane the aircraft follows the trajectory, while the bank angle command limit decreases linearly with height above ground to ensure a wings level touchdown. At a fixed height, the aircraft conducts a de-crab maneuver to align the aircraft heading with the runway track in case of crosswind. In case the height increases during the pitch control phase due to atmospheric disturbances, the landing phase returns to flare. Thereby, the vertical speed and airspeed is actively controlled in order to prevent entering a low energy state or even stalling the aircraft close to ground.

De-rotation After touchdown the de-rotation phase becomes active. The WoW sensors on the left and right main landing gear detect the touchdown. Both sensors need to exceed a threshold value for multiple consecutive time-steps in order to change the internal aircraft state from airborne to on-ground. In the vertical plane the pitch angle is decreased to put the nose wheel slowly on the ground. Since there is no WoW sensor for the nose wheel, the de-rotation is completed when the measured pitch angle is below a predefined threshold. The heading controller is used to maintain the runway heading. The ailerons are faded to the centered position

Roll-out When the de-rotation is completed, the roll-out phase is activated. During roll-out, the runway centerline is tracked by the ground controller. The elevator is faded a default position. As there are no automatic brakes on the aircraft, the pilot then disengages the AFCS and decelerates the aircraft to a standstill.

4 Take-off and Landing Simulation

In order to test the integrated ATOL module and to analyse the safety and robustness of the automated take-off and landing maneuvers, suitable test cases were defined and evaluated using software-in-the-loop (SIL) and aircraft-in-the-loop (AIL) simulations. All maneuvers for the flight tests, including the AFCS tests were first simulated in the SIL and then in the AIL environment to ensure the desired behavior and the safety of the maneuvers.

4.1 Simulation Model

An integration simulation model consisting of an flight dynamics model (FDM), models of flight control components such as sensors and actuators as well as the AFCS functional algorithms was implemented in order to the the automatic take-off and landing functions. The FDM is a six degree of freedom aircraft model, including models for static and dynamic atmosphere and terrain. Further, relevant aircraft subsystems such as the landing gear or the aerodynamic ground effect were modelled. The integration model also contains models for all sensors. These models include the dynamic behaviour, discretization effects and their respective interfaces to generate appropriate data inputs for the control algorithms. Commands for the AFCS or pilot control inputs can be send to the simulation

AUTOMATIC TAKE-OFF AND LANDING OF A VERY LIGHT ALL ELECTRIC OPTIONALLY PILOTED AIRCRAFT

for closed-loop programmed or manually flown test cases. The simulation outputs were used for data logging and visualization in *X-Plane*, see figure 7.

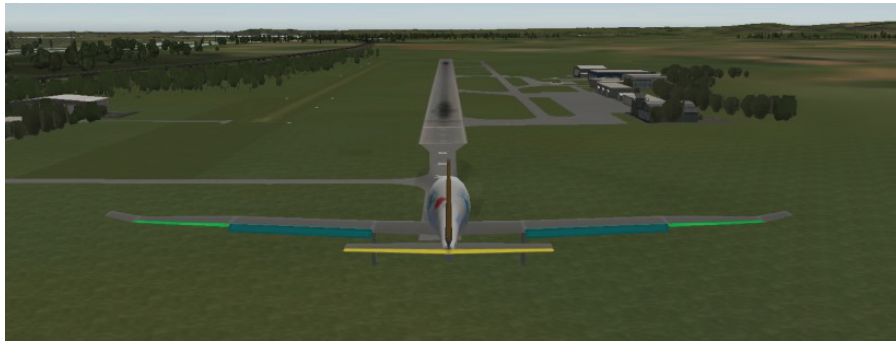


Figure 7 – Visualization of a simulated landing in *X-Plane*

4.2 ATOL Simulation Testing

Testing via simulation was conducted to verify the safety of the designed take-off and landing maneuvers. Therefore the parameters for runway direction, approach angle, initial position, as well as static wind and turbulence were varied. A set of varying wind and turbulence parameters were used to test the take-off and landing algorithms. Figure 8 shows a simulated take-off maneuver with atmospheric disturbance characteristics which were comparable to the disturbances observed in previous flight tests.

The commands are shown in magenta, the measurements in blue. In addition the kinematic speed is shown in green. The change of the take-off phases is indicated by vertical lines. The aircraft accelerates with maximum thrust. After reaching the rotation speed the feed-forward elevator rate command initiates the rotation. When the rotation phase begins, the pitch angle command increases starting from the current measurement to the target value. The pitch angle is then held until the climb height is reached. In the following climb phase the autopilot is activated, and the aircraft performs an open climb.

Figure 9 shows the final phases of a simulated landing maneuver with active disturbance and wind. During the final approach the aircraft follows the landing trajectory. At the beginning of the flare, the vertical control switches to a constant vertical speed command. Right before touchdown, the pitch control phase is activated, to increase the pitch attitude for landing. The pitch command starts at the current measurement and increases to its target value. Since the pitch angle is lower than the threshold to end the de-rotation, this phase is skipped. The phase changes directly to roll-out, since the pitch angle is below the predefined threshold to exit the de-rotation phase.

4.3 Aircraft-in-the-Loop Tests

Before each flight test, the scheduled test points were conducted in an AIL environment. In this setup, the complete flight control system can be tested using the actual hardware components and interfaces. The AIL simulation was realized through simulating the FDM and sensor characteristics on an industrial real-time computer and injecting the virtual sensor signals through the real interfaces to the aircraft systems. In order to simulate the response of the aircraft due to inputs from the pilot or the flight control system, the measured control surface positions were used as input for the FDM.

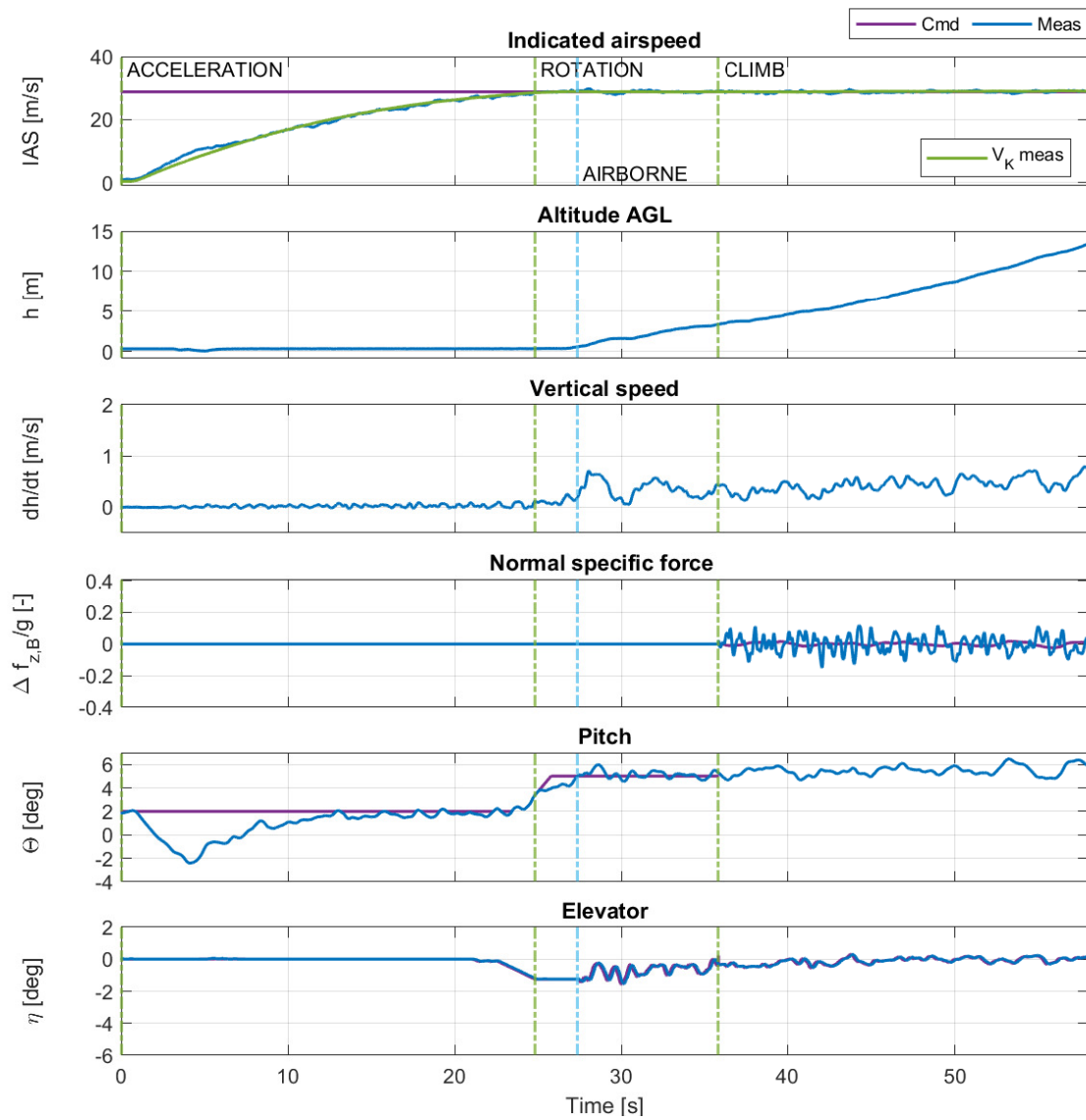


Figure 8 – Take-off simulation results

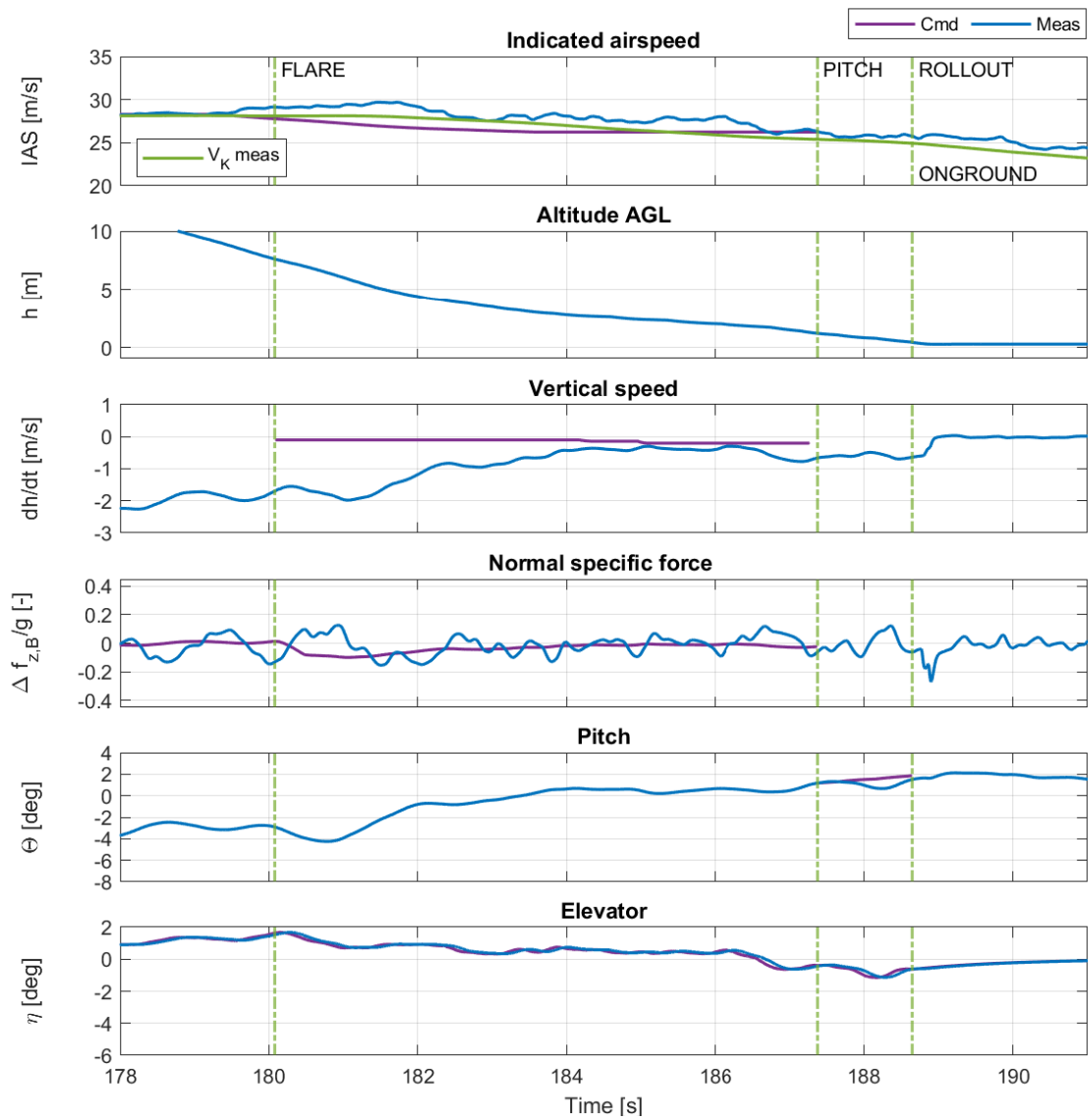


Figure 9 – Landing simulation results

5 Flight Tests

Flight tests were performed to assess the AFCS performance for different flight modes required as basis for ATOL. These modes are lateral and vertical trajectory control, vertical speed control as well as speed by thrust or pitch. Finally, flight tests were performed to successively test the automatic take-off and landing control functions. All flight tests were conducted at the airfield *EDML* close to Munich. The airfield has a tarmac runway with 900 m length.

5.1 Ground Tests

Initial ground roll tests showed that the control authority of the rudder at low speeds was not sufficient to counteract the yaw moment induced by the propeller at full thrust. Due to that reason, the rudder control was disengaged by opening the clutch during take-off until the climb phase as well as shortly after touchdown when landing. In both cases the pilot manually controlled the aircraft direction on ground using rudder and differential brakes to ensure centerline tracking, while the AFCS controlled the elevator, aileron and throttle.

5.2 Autopilot and Trajectory Control

Figure 10 shows the flight data with active trajectory control. The example flight plan consists of five waypoints. The transition between the waypoints is specified as fly-by (type 0). Alternatively, also fly-over waypoints would be possible. As described in section 2.1, the waypoints are connected by straight lines as indicated by the magenta dotted lines. After activation of the trajectory mode, the first straight line segment is defined from the current aircraft position (*WP 0*) to the first next-waypoint (*WP 1*). Since the initial heading does not allow a direct flight towards this waypoint, a capture maneuver was flown. The other waypoints specify a traffic pattern like trajectory with an overflight of the runway at constant altitude. The aircraft flight path shows a good tracking of the desired trajectory including appropriate fly-by transitions between the segments. All waypoints are located at the same altitude of 609.6 m (2000 ft) MSL. The altitude was tracked with an accuracy of less than 5 m. The desired airspeed for the complete waypoint list was set to the nominal en-route speed of 28.3 m/s (55 kt). A tracking accuracy of less than 2 m/s was achieved.

The initial closed-loop flight control performance was greatly affected by nonlinear transmission effects in the electro-mechanical flight control systems. These effects resulted in deficiencies in closed-loop control performance, such as small oscillations and insufficient tracking performance. The closed-loop control performance could be improved by adding a nonlinear command compensation algorithm as shown in [21]. The compensation was active during all flight tests shown in this paper.

5.3 High Altitude ATOL Maneuvers

Flare in the air

In order to test the performance of the flare, the maneuver was tested in high altitude in landing configuration with flaps and gear extended. The flare test maneuver was executed automatically by the FCC. First a descent with an glide path of -4° was commanded. When the descent was stabilized, the flare mode of the AFCS was activated to reduce the rate of descent from approx. -2 m/s to -0.3 m/s. Figure 11 shows the result of a flight test.

Pitch control

In order to validate the pitch controller tracking behavior, dedicated tests in landing configuration were performed at high altitude. For these tests, a pitch doublet command was injected by the FCC. The demonstrator aircraft flies with negative pitch angle during steady straight and level flight, when in landing configuration. Figure 12 shows the result in a flight test.

5.4 Automatic Take-off

The automatic take-off could be demonstrated in a flight test. Figure 13 shows the results of the flight test. Compared to the simulation results in section 8, the behaviour was as expected with small differences.

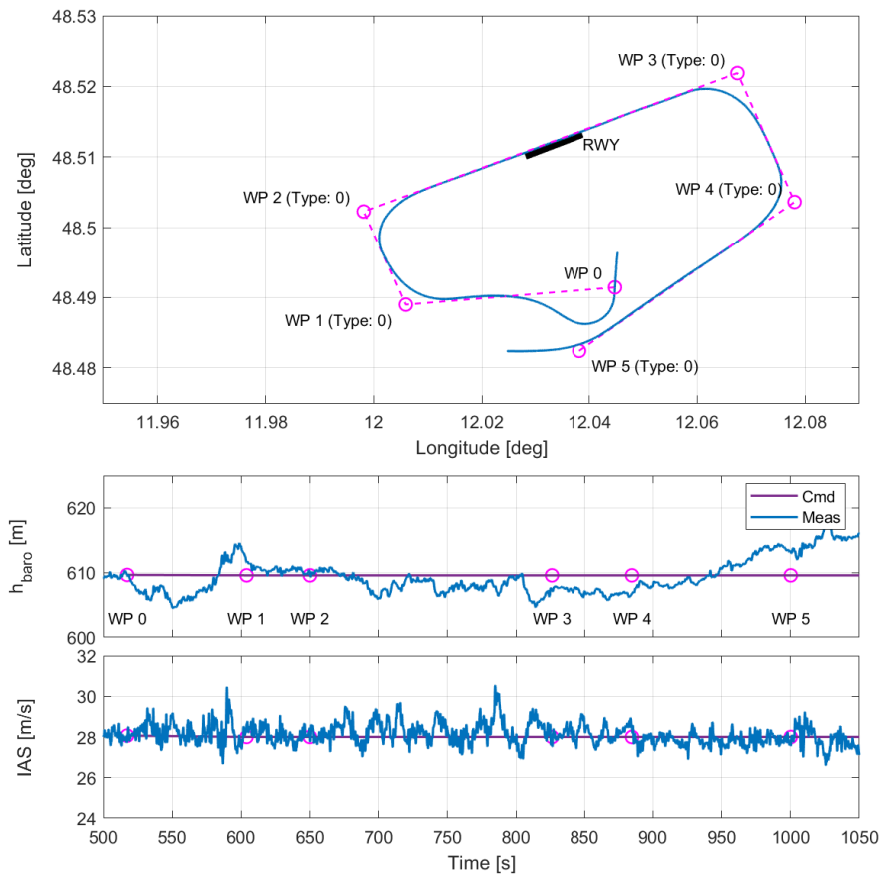


Figure 10 – Trajectory flight test

As indicated by the blue vertical line, the internal aircraft state changed to airborne during the acceleration phase. As described in section 3, in this case the pitch controller is activated with a predefined pitch angle command to further accelerate close to ground. The high frequency disturbance in the pitch angle can be explained by rolling over small runway bumps at high ground speed, as the main wheels are initially still on ground with little load below the threshold for on-ground detection. As the pitch controller is active, the disturbance is damped by the controller.

With the commanded small pitch angle, the aircraft reaches the climb height, before the designed rotation speed was reached. Therefore the phase changes directly from acceleration to climb. Due to uncertainties in the aerodynamic ground effect of the FDM, the additional lift close to ground was larger than expected. However the command generation and state machine of the take-off maneuver were designed to handle the event and conducted a safe maneuver in flight test.

5.5 Automatic Landing

After testing the different control laws required for the automatic landing, multiple approaches were performed with decreasing lower minimum go-around altitudes to successively validate the automatic landing maneuver and the overall controller performance, before finally multiple complete landings until touchdown were performed.

Figure 14 shows the trajectory of an automatic landing flight test. The landing was activated at *WP 0*. The first waypoint (*WP 1*) is specified as loiter waypoint where the aircraft starts a right-hand loiter maneuver until the landing is confirmed by the operator from the GCS. In the shown example, the landing was confirmed shortly after start of the loiter, resulting in a clearance for continue the landing. The remaining two waypoints (*WP 2/3*) represent the initial approach leg and are required to align the aircraft track with the landing trajectory on the FCC. Between the last two waypoints, the aircraft intersects the landing trajectory which causes the initiation of the automatic landing as described in section 3.5. The aircraft descends on the trajectory with a flight path angle of -4° until flare and

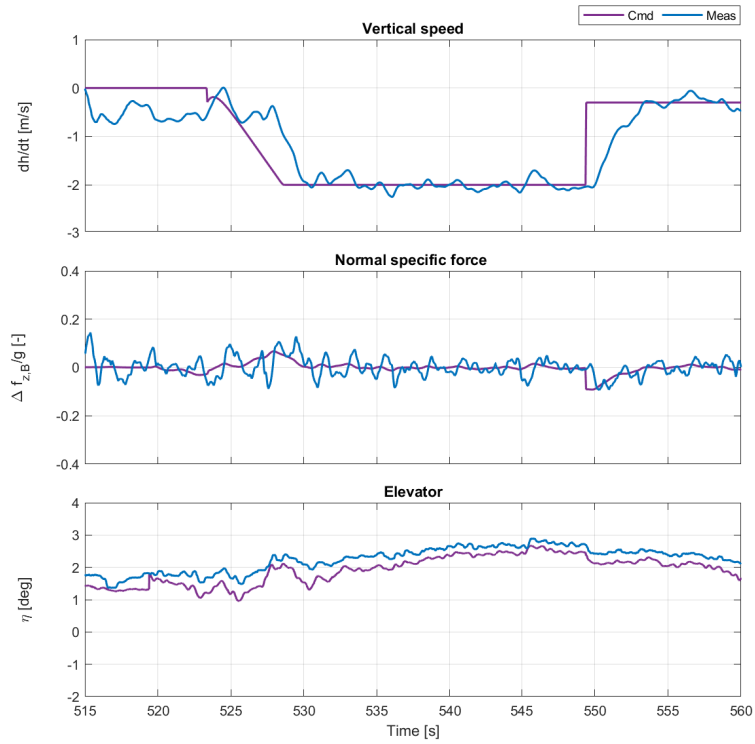


Figure 11 – Flare in the air flight test results

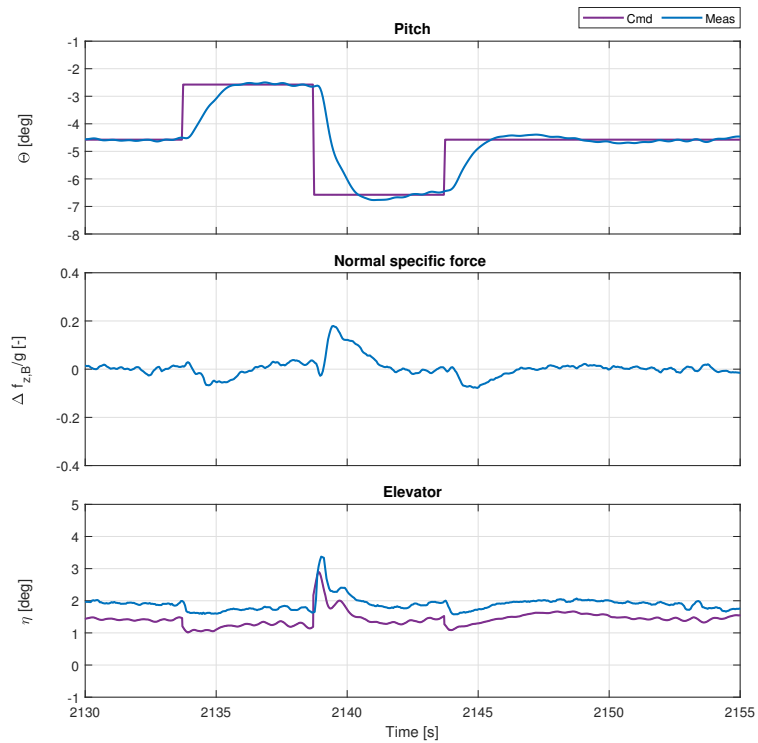


Figure 12 – Pitch controller flight test results

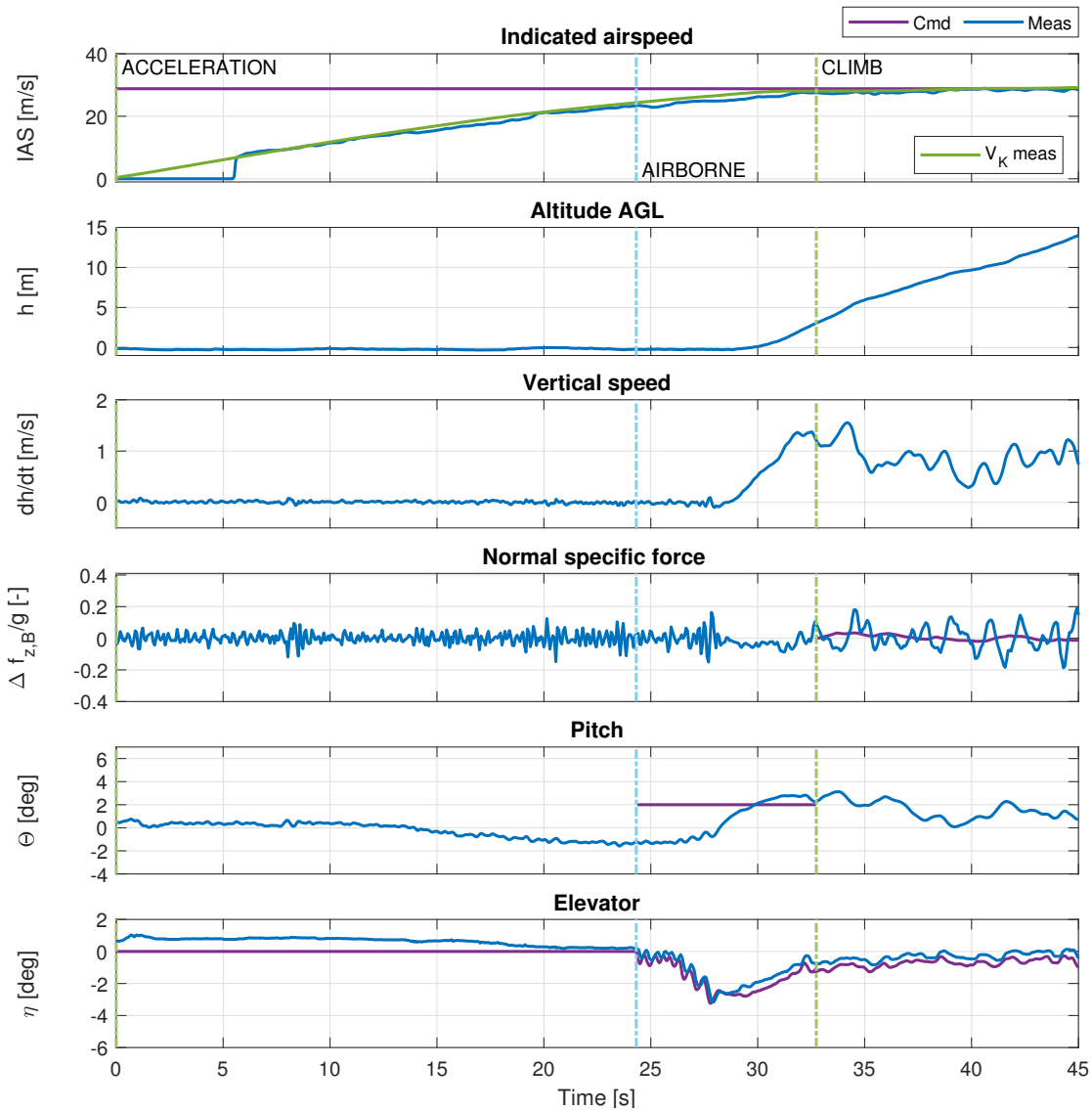


Figure 13 – Take-off flight test results

touchdown. The target speed was held constant at 28.3 m/s (55 kt) during the descent. A slight increase in airspeed results due to the steep approach while the throttle is almost in idle position.

Figure 15 shows the final approach until touchdown. The airspeed command during final approach was set 28.3 m/s (55 kt). Compared to the landing simulation in figure 9, similar results with small differences could be observed. Since the response of the vertical speed controller was faster during flight test compared to simulation, the flare time was longer. Furthermore at the beginning of the pitch control phase the initial pitch angle was lower compared to simulation. This can also be explained by uncertainties in the aerodynamic ground effect, as the negative induced pitch moment was slightly higher than expected. However during the pitch control phase the nose was lifted up and a safe landing on the main landing gear was ensured. As the pitch angle at touchdown was below the threshold for exiting the de-rotation phase, the phase changed immediately to roll-out. The pilot then disengaged the AFCS.

Figure 16 shows a picture from the belly camera of the demonstrator aircraft right before touchdown during an automatic landing.

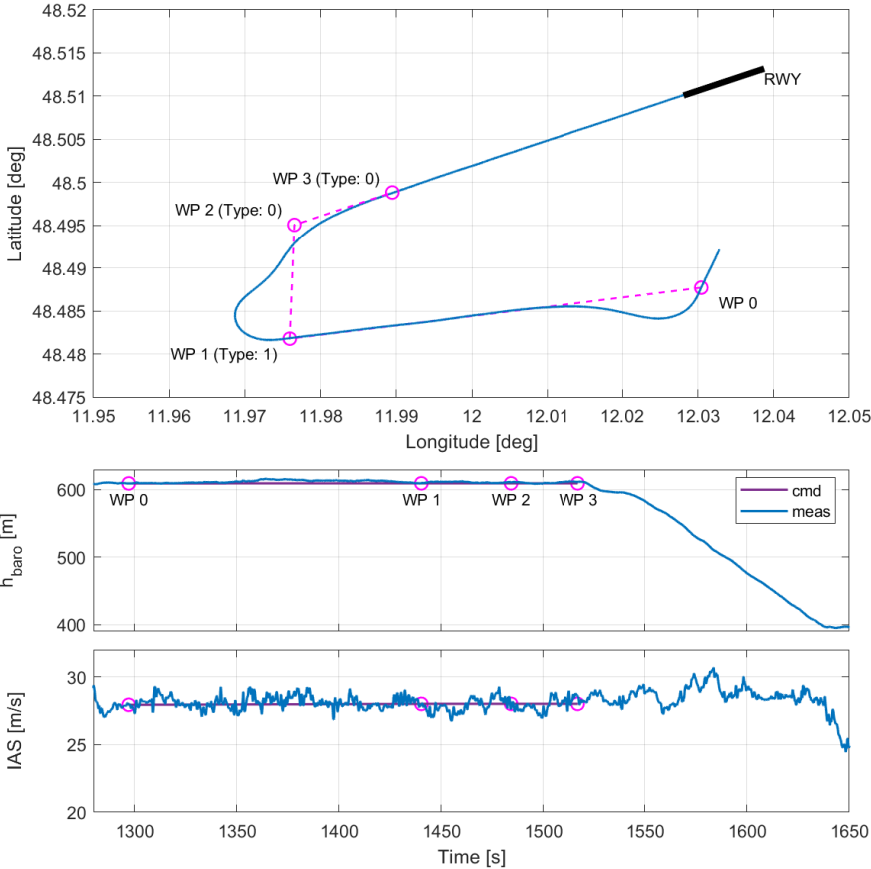


Figure 14 – Initial approach and landing trajectory flight test results

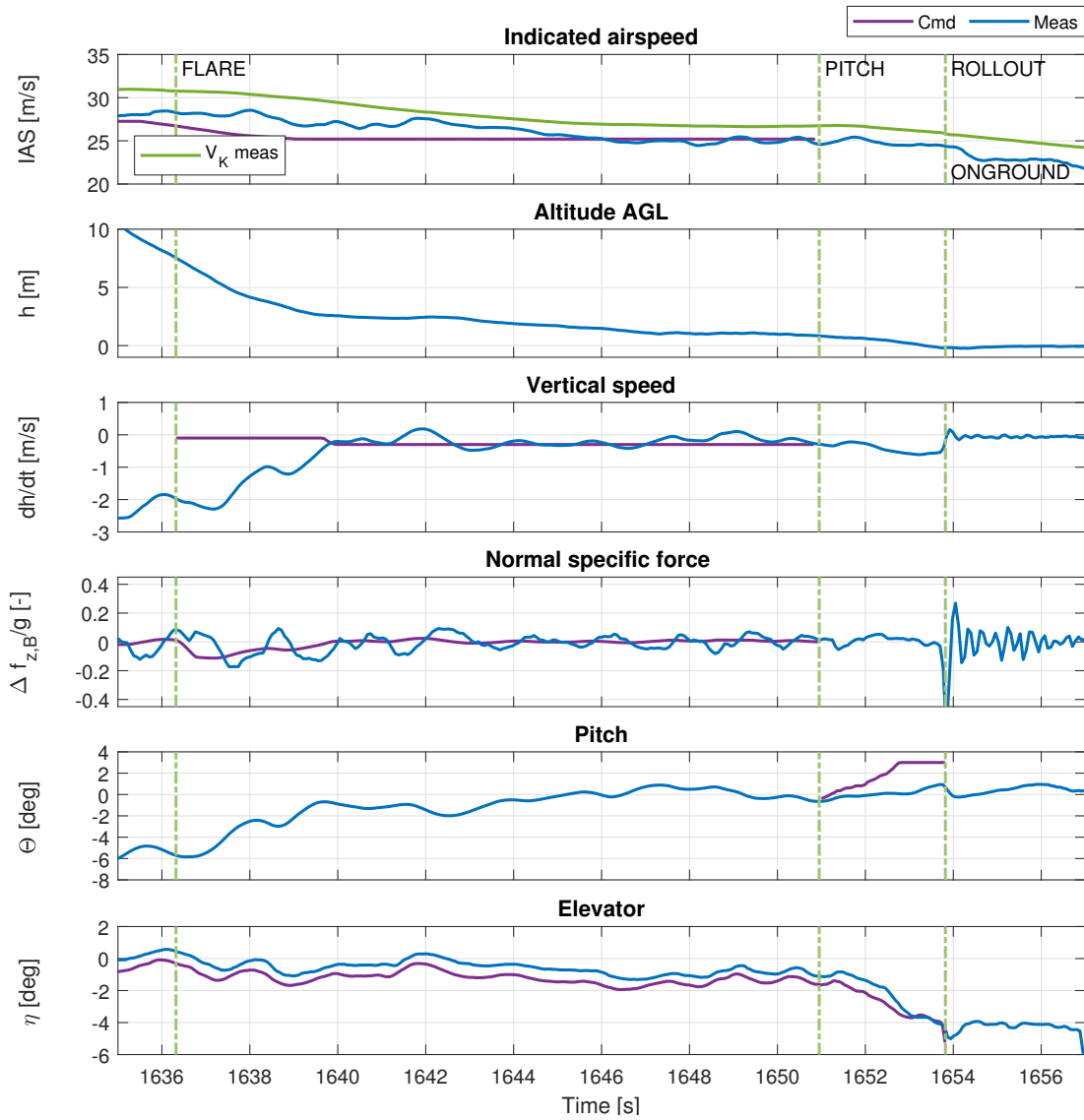


Figure 15 – Landing flight test results



Figure 16 – Aircraft during automatic landing before touchdown

6 Conclusion

An automatic take-off and landing system was designed, developed and demonstrated for a very light all-electric optionally-piloted aircraft. A step-wise approach to design and test the sub-maneuvers was conducted. Simulation results as well as real flight test data demonstrated a successful automatic take-off and landing of the demonstrator aircraft.

Future work should focus on developing a more accurate model of the aerodynamic ground effect in order to optimize the model-based design of the take-off and landing functions. Adding a nose wheel steering actuation to the aircraft would enable the control of the yaw axis on ground and therefore automatic centerline tracking during the take-off run. Automatic control of flaps and gear would further increase the degree of automation to extend the aircraft capabilities towards full OPV operation.

Acknowledgment

Part of this work was funded by the Bavarian Ministry of Economic Affairs within the *AURAS* research project (funding number: LABAY90D).

Gefördert durch

Bayerisches Staatsministerium für
Wirtschaft, Landesentwicklung und Energie



We would like to thank our colleagues Martin Kügler and Christoph Krause from the Institute of Flight System Dynamics for previously working on the test platform and enabling this work. We also would like to thank Ferdinand Settele from Hochschule München for his contributions on the FMC.

6.1 Author Information

Simon Scherer: simon.scherer@tum.de

7 Copyright Statement

The authors confirm that they, and/or their company or organization, hold copyright on all of the original material included in this paper. The authors also confirm that they have obtained permission, from the copyright holder of any third party material included in this paper, to publish it as part of their paper. The authors confirm that they give permission, or have obtained permission from the copyright holder of this paper, for the publication and distribution of this paper as part of the ICAS proceedings or as individual off-prints from the proceedings.

References

- [1] EASA, “All weather operations (CS-AWO),” 2018.
- [2] “Smartpath, the first and only GBAS solution certified by the FAA.” <https://aerospace.honeywell.com/content/dam/aerobt/en/documents/learn/products/navigation-and-radios/brochures/C61-1663-000-000-SmartPathPrecisionLandingSystem-bro.pdf>. Accessed: 2022-05-31.
- [3] Airbus, “Airbus concludes ATTOL with fully autonomous flight tests (press release),” 2020.
- [4] T. Bernard and B. Tuccio, “Garmin autoland: Simulator and flight testing of an emergency autonomous landing system,” in *Society of Flight Test Engineers International Symposium*, 2020.
- [5] Xwing. <https://www.xwing.com/>. Accessed: 2022-05-30.
- [6] M. Lamp and R. Luckner, “Automatic landing of a high-aspect-ratio aircraft without using the thrust,” in *Advances in Aerospace Guidance, Navigation and Control*, pp. 549–567, Springer, 2015.
- [7] F. Pinchetti, J. Stephan, A. Joos, and W. Fichter, *FlySmart-Automatic Take-Off and Landing of an EASA CS-23 Aircraft*. Deutsche Gesellschaft für Luft-und Raumfahrt-Lilienthal-Oberth eV, 2016.
- [8] N. C. Mumm and F. Holzapfel, “Development of an automatic landing system for diamond da 42 aircraft utilizing a load factor inner loop command system,” in *CEAS EuroGNC*, 2017.
- [9] A. W. Zollitsch, N. C. Mumm, S. Wulf, F. Holzapfel, M. Hochstrasser, P. J. Lauffs, and L. Peter, “Automatic takeoff of a general aviation research aircraft,” in *11th Asian Control Conference (ASCC)*, pp. 1683–1688, 2017.
- [10] M. E. Kügler, M. Heller, and F. Holzapfel, “Automatic take-off and landing on the maiden flight of a novel fixed-wing uav,” in *Flight Testing Conference*, 2018.

- [11] C. Krause, *Safe and Robust Automation of Aircraft and System Operation*. Dissertation, Technische Universität München, München, 2020.
- [12] M. E. Kügler and F. Holzapfel, "Autoland for a novel UAV as a state-machine-based extension to a modular automatic flight guidance and control system," in *American Control Conference (ACC)*, pp. 2231–2236, IEEE, 2017.
- [13] C. Krammer, C. Mishra, and F. Holzapfel, "Testing and Evaluation of a Vision-Augmented Navigation System for Automatic Landings of General Aviation Aircraft," American Institute of Aeronautics and Astronautics.
- [14] E. Karlsson, S. P. Schatz, T. Baier, C. Dörhöfer, A. Gabrys, M. Hochstrasser, C. Krause, P. J. Lauffs, N. C. Mumm, K. Nürnberger, L. Peter, V. Schneider, P. Spiegel, L. Steinert, A. W. Zollitsch, and F. Holzapfel, "Development of an Automatic Flight Path Controller for a DA42 General Aviation Aircraft," in *Advances in Aerospace Guidance, Navigation and Control*, pp. 121–139, 2018.
- [15] E. Karlsson, S. P. Schatz, T. Baier, C. Dörhöfer, A. Gabrys, M. Hochstrasser, C. Krause, P. J. Lauffs, N. C. Mumm, K. Nürnberger, L. Peter, V. Schneider, P. Spiegel, L. Steinert, A. W. Zollitsch, and F. Holzapfel, "Automatic flight path control of an experimental da42 general aviation aircraft," in *14th International Conference on Control, Automation, Robotics and Vision (ICARCV)*, pp. 1–6, 2016.
- [16] C. Krause and F. Holzapfel, "Designing and implementing a clutch automation for a fully electric fixed-wing opv," in *2nd International Conference in Aerospace for Young Scientists (2nd ICAYS)*, pp. 1–8, 2017.
- [17] C. Krause and F. Holzapfel, "Designing a system automation for a novel uav demonstrator," in *2016 14th International Conference on Control, Automation, Robotics and Vision (ICARCV)*.
- [18] D. Seiferth, R. Kuchar, and M. Heller, "Model-based design and real live on-runway testing of a ground controller for a novel diamond-shaped unmanned air vehicle (uav)," in *2017 IEEE 56th Annual Conference on Decision and Control (CDC)*, pp. 3934–3941, IEEE, 2017.
- [19] S. P. Scherer, C. Mishra, and F. Holzapfel, "Extension of the capabilities of an automatic landing system with procedures motivated by visual-flight-rules," in *33rd Congress of the international council of the aeronautical sciences*, 2022. Submitted for publication.
- [20] N. C. Mumm, V. Schneider, and F. Holzapfel, "Nonlinear continuous and differentiable 3d trajectory command generation," in *IEEE international conference on aerospace electronics and remote sensing technology (ICARES)*, IEEE, 2015.
- [21] S. P. Scherer, M. Speckmaier, D. Gierszewski, A. Steinert, and F. Holzapfel, "Compensation of nonlinear transmission effects in electro-mechanical flight control systems," in *AIAA SciTech 2022 Forum*, 2022.